Cell-Based Dose Responses from Open-Well Microchambers
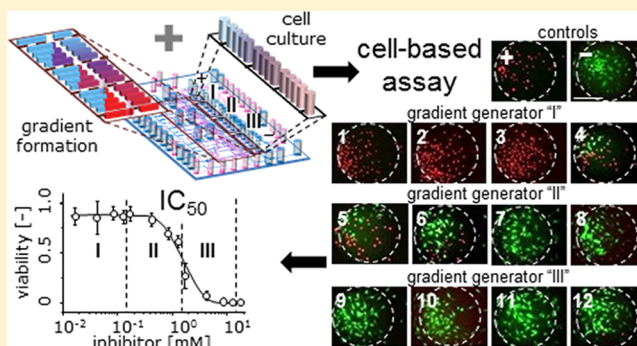
Morgan Hamon,[†] Sachin Jambovane,[†,∇] Lauren Bradley,[†] Ali Khademhosseini,[‡,§,∥,⊥] and Jong Wook Hong*,[†,#]

[†]Materials Research and Education Center, Department of Mechanical Engineering, Auburn University, Auburn, Alabama 36849, United States

[‡]Center for Biomedical Engineering, Department of Medicine, Brigham & Women's Hospital, Harvard Medical School, Boston, Massachusetts 02115, United States

[§]Harvard-MIT Division of Health Sciences and Technology, Massachusetts Institute of Technology, Cambridge, Massachusetts 02139, United States

[∥]Wyss Institute for Biologically Inspired Engineering, Harvard University, Boston, Massachusetts 02115, United States

[⊥]Department of Maxillofacial Biomedical Engineering, Institute of Oral Biology, School of Dentistry, Kyung Hee University, Seoul, Korea

[#]College of Pharmacy, Seoul National University, Seoul, 151-741, Korea

S *Supporting Information*

ABSTRACT: Cell-based assays play a critical role in discovery of new drugs and facilitating research in cancer, immunology, and stem cells. Conventionally, they are performed in Petri dishes, tubes, or well plates, using milliliters of reagents and thousands of cells to obtain one data point. Here, we are introducing a new platform to realize cell-based assay capable of increased throughput and greater sensitivity with a limited number of cells. We integrated an array of open-well microchambers into a gradient generation system. Consequently, cell-based dose responses were examined with a single device. We measured IC_{50} values of three cytotoxic chemicals, Triton X-100, H_2O_2, and cadmium chloride, as model compounds. The present system is highly suitable for the discovery of new drugs and studying the effect of chemicals on cell viability or mortality with limited samples and cells.

The development of a new drug requires selection of drug candidates, preclinical tests, and clinical trials.[1] In the selection process or the target molecule discovery step, potential drug targets to a disease are identified[2,3] and banks of drug candidates are tested,[4,5] resulting in lead compounds.[6,7] During the course of identifying the lead compound, cell-based dose responses or the half-maximal inhibitory concentrations (IC_{50}) of target molecules are essential[5,8−10] to bridge the gaps between molecular assays and animal tests.[11]

Conventionally, to measure cellular IC_{50}, target cells are cultured in vitro and exposed to a wide range of concentrations of the candidate in a linear or logarithmic dilution series[12] to confirm the effect of the different concentrations on the cellular growth and function.[13] For this purpose, thousands of cells from target organs are cultured and treated with various chemicals in Petri dishes, flasks, or well plates[14] by consuming milliliters of reagents. Then a dose−response curve is plotted from which the IC_{50} value is determined.[12,13,15] Obviously, with this method, it is hard to conduct parallel experiments, especially with rare and precious samples. As an alternative, 96-well plates are used.[16] Although this method reduces the volume of reagents for each test down to submilliliters, it still

requires relatively large amounts of samples. For more efficient drug development with less volume of reagents, microfluidic systems have been reported,[17] and particularly for IC_{50} experiments, a cellular microarray is introduced to host thousands of tests in one experiment.[18] However, to minimize potential cross-contamination across the cells and the target molecules, acute sandwiching of two slides for a cell plate is required.[19] Recently, trials to measure IC_{50} on a fluidic format have been examined[20−22] with a limited concentration gradient, 0−50 μM, through continuous supply of reagents over 12 chambers. In this case, shear stress to cells from the flow could influence IC_{50} values.[23,24] In addition, cells are likely to get damaged during the introduction step because they must travel through microchannels. Tubeless microfluidic systems using a passive pumping method[25] have been used to minimize cell damages and control shear stress on adherent cells.[26] Despite
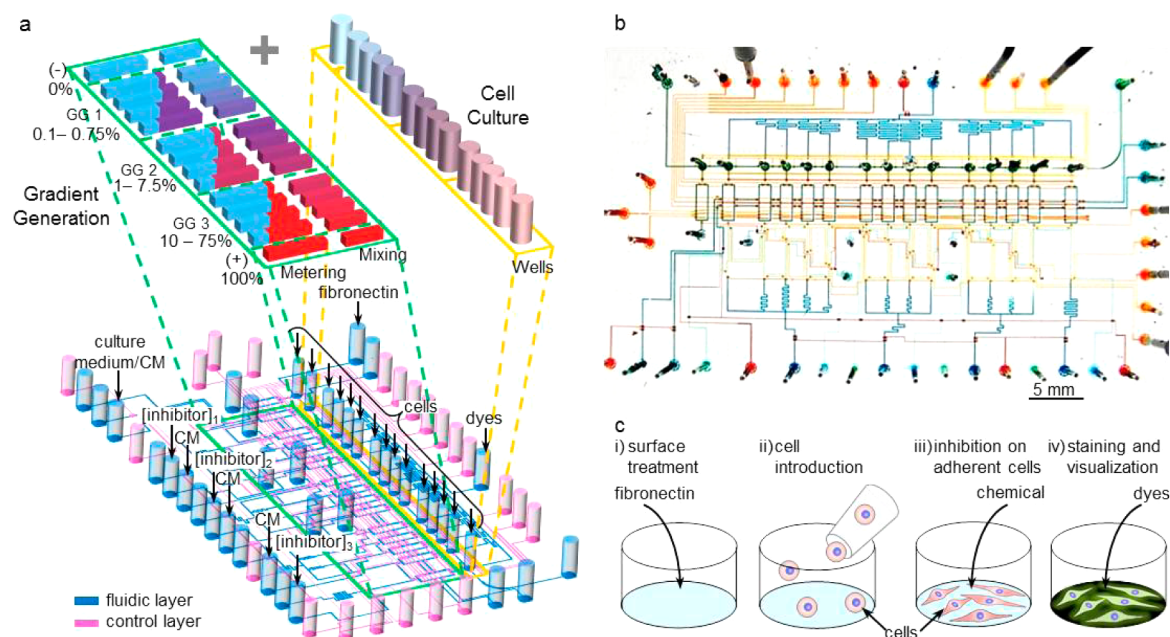
Figure 1. System outline and step-by-step processes of cell handling. (a) Three-dimensional schematic representation of the system. The fluidic channels and the wells are colored in blue. The control channels are colored in pink. Inlets for culture medium (CM), inhibitors at different concentrations (1, 2, and 3), fibronectin, and cells are indicated. Close-ups show the cell culture system and the gradient generation system. (b) Actual picture of the present system. Channels and wells are filled with food dyes of red, orange, yellow, blue, sky blue, and green on the basis of the functionality. (c) Step-by-step processes of the cell handling. (i) The bottom surfaces of the wells are coated with fibronectin. (ii) Then cells are introduced to the microwells. (iii) Through the gradient formers, chemicals of interest are introduced into the wells, (iv) followed by live/dead cell imaging.

these advantages,[27] they require precise sample handling by laborious pipetting or large automated liquid handlers.[27]

We report cell culture and cytotoxicity assays in nanoliter-scale microchambers through a novel integration of our log-scale gradient generators (GGs)[28−30] and open-well micro-structures. This integration also enables direct introduction of cells from the top of the open wells, resulting in faster and more homogeneous distribution of cells.

■ MATERIALS AND METHODS

Chip Design and Fabrication. The microfluidic chip has three GGs, and each GG is composed of four processors as shown in Figure 1a. Every GG unit is divided into a metering section, a mixing section, and a cell culture section. All these sections are separated with a pneumatic microvalve. The dilution ratio of the inhibitor is determined by the ratio of the lengths of the metering channel of each processor. The detailed design and configuration of the chip is depicted in the Supporting Information, Figure S1. The flow channels are 100 μm wide and 20 ± 0.5 μm high. The width of the control channels is 50 μm except for the valve areas. For shutoff valves and mixing valves, the width is typically 200 μm. We fabricated the chip with standard multilayer soft lithography methods following detailed conditions used in our previous studies[28−32] and by others.[33−36]

Gradient Formation. To generate a concentration gradient over the 14 microchambers, we borrowed the chip design and the operation steps as described in our previous paper.[30] In each GG, final concentrations of 75%, 50%, 25%, and 10% of the originally introduced solution concentration can be generated (Supporting Information, Figure S1). If we introduce, for example, 10× inhibitor and 1× working buffer to a GG, we can create concentration points of 1×, 2.5×, 5×,

and 7.5×. Likewise, if we feed 10× inhibitor to the first GG (GG1), 100× to GG2, and then 1000× to GG3, the effective concentrations will be 1×, 2.5×, 5×, 7.5×, 10×, 25×, 50×, 75×, 100×, 250×, 500×, and 750×, including 0 negative control and 1000× for the positive control. The diluted chemicals in the GGs are pushed, then, to the microwell chambers, resulting in further dilution of the solutions.

To confirm the generation of a logarithmically increased concentration gradient in the microwell chambers, we introduced carboxyfluorescein (FAM) into the three GGs at initial concentrations of 1, 10, and 100 μM. We then pushed the solutions from the metering section into the mixing section, where peristaltic mixing of the metered FAM solutions occurred with distilled water. Finally, the mixed and diluted fluorescent molecules were delivered into the wells, resulting in 100-fold-diluted FAM. We measured the fluorescence intensity in each well with a modified biochip scanner (arrayWoRx, Applied Precision, Issaquah, WA). The experiment was repeated three times with three different chips.

Device Operation. The step-by-step operation includes surface treatment of the microwells, introduction of the cells, culture of the cells with the inhibitor, and live/dead cell assay (Figure 1c (i−iv) and Supporting Information, Figures S2−S4). Although the operation for one cell chamber is described, all fourteen processors are operated simultaneously.

Surface Treatment and Introduction of Cells. A solution of 50 μg of fibronectin (Invitrogen, Grand Island, NY) in 1 mL of PBS (Sigma, St. Louis, MO) was used to coat the surfaces of the microwells through the "fibronectin channel" (see the Supporting Information, Figure S1, for valve and channel positions and names) followed by overnight incubation at 37 °C. After incubation, the solution of fibronectin was removed from the microwells and cells were introduced. To prevent

formation of air bubbles during the introduction of the solution, the device was first degassed in a 75 mmHg vacuum pump for 2 h prior to the introduction of the solution.

Cell Culture and Cytotoxicity Tests. NIH/3T3 cells (American Type Culture Collection (ATCC), Manassas, VA) were cultured in 25 cm² flasks (VWR, Radnor, PA) in Dulbecco's modified Eagle's medium (DMEM; ATCC) complemented with 10% calf serum (ATCC) and 1% antibiotic/antimycotic (Invitrogen). Cells were grown in a humidified incubator at 37 °C and supplemented with 5% CO₂. The culture medium was changed every two days. The cells were subcultured when reaching 50−75% confluence.

For on-chip experiments, we autoclaved the device to sterilize the microchambers (45 min, 121 °C). Cells were washed twice with PBS, detached with warm 0.25% trypsin/ EDTA solution (Invitrogen), counted, and resuspended in 1 mL of DMEM culture medium, making the final cell concentration ~2 × 10⁵ cells/mL. For each microwell, we introduced cells manually from the top of the microwell with a 275−300 µm diameter pipet tip (Bio-Rad, Hercules, CA). For each microwell a different tip was used. After cell introduction into the 14 microwells, we closed the surrounding valves and put the whole chip in a humidified incubator (37 °C, 5% CO₂). After 2 h, inhibitors at different concentrations were introduced into the microwells.

Live/Dead Cell Assay. After 24 h of exposure to the inhibitor, we replaced the culture medium with fresh medium that contained calcein AM (15 µM; Sigma-Aldrich, St. Louis, MO), for live cell staining, and propidium iodide (1.5 µM; Invitrogen), for dead cell staining. Cells were then incubated for 20 min and visualized under a fluorescent microscope with a 10× objective lens. We counted dead and live cells and determined the cell viability in each well.

Off-Chip Cell Cytotoxicity. For off-chip cytotoxicity, experiments were done in 96-well plates. Cells were washed twice with PBS and detached with warm 0.25% trypsin/EDTA solution (Invitrogen). We counted the cells and resuspended them in 1 mL of DMEM culture medium at a concentration of 5 × 10⁴ cells/mL. We introduced 100 µL of cell suspension to each well. After cell attachment and spreading, we replaced the culture medium with 100 µL of inhibitor solution composed of culture medium. Different concentrations of inhibitors CdCl₂, H₂O₂, and Triton X-100 were provided. After 24 h of culture, 100 µL of culture medium, calcein AM (15 µM final concentration) and propidium iodide (1.5 µM final concentration), was added into the wells. For each well, we took pictures and the viability was calculated.

Statistical Analysis. IC_{50} values were determined through curve-fitting of the four-parameter nonlinear-logistic-regression model based on the obtained inhibition data. In the present work, we used the following four-parameter model:[30,37]

$$I = I_{min} + \frac{I_{max} - I_{min}}{1 + 10^{(\log(IC_{50}) - [I])h}}$$

where [I] represents the concentration of inhibitor, I designates the inhibiting potency (%), including the minimum (I_{min}, %) and maximum (I_{max}, %), and h is the Hill coefficient or Hill slope, which represents the steepness of the dose−response plot.

■ RESULTS AND DISCUSSION

Chip for Systematic Cell Assay. The microwell chamber designed for conducting the cell-based assay is a characteristic feature of our device. The majority of existing cell culture microdevices use complex channel networks and cell arresters, which could constrain the proper growth of cells and cause damage due to shear stress to the cells. To avoid these problems of existing approaches, we envisioned open microwell chambers. Although open microchambers have previously been described,[38−40] this is, to our knowledge, the first time that such structures have been used for long-term culture of cells in a microscale batch system. We found that open microwell chambers were simple and effective ways to provide adequate amounts of medium for long-term cell culture compared to the continuous-flow-based fluidic system,[21,22] which consumes up to several milliliters of samples. Our system requires only nanoliters of samples with a limited number of cells, ~100−150 cells per microwell (Table 1). Each microwell chamber contains

Table 1. Comparison of the Present System and Existing Continuous-Flow-Based Systems for Cell-Based Assay

	present open-well microfluidic system	existing continuous-flow microfluidic systems[21,22]
number of cells (per chip)	~1400−2100	~3600−80000
throughput (per chip)	14 × 1	10 × 5 or 12 × 1
flow rate	NA	1.3−30 µL/h
sample volume	~14 µL	300 µL to 1 mL

a reaction volume of approximately 900 nL, providing enough glucose to culture hundreds of cells for several days of the experiment. The microwell chambers for cell introduction and culture are connected to 14 parallel processors (Figure 1 and Supporting Information, Figure S1).

One critical advantage of the present system is that the cells are directly introduced from the top of the open wells. One of the crucial yet difficult steps to harbor cells into microchannels or microchambers is the reliable and reproducible introduction of cells into the loci. Typically, for this, the cells should land, anchor, spread, and proliferate[20,41] inside the microwell. Although mechanical trapping of the cells has been previously described to immobilize cells in microchambers,[42−45] such methods are poorly suited for mammalian cells because of the potential damage of cells caused by mechanical stresses. Instead, in our device, we introduced the cells into the wells from the top opening. In addition, we could not observe any hampered cell growth that is commonly observed when cells are maintained in microchambers or microchannels.[46,47] Through the direct introduction, we confirmed a homogeneous distribution of cells across the microchambers (coefficient of variation (CV) of 14 ± 5). On the other hand, when the cells were introduced through microchannels, the cell distribution was random (CV = 44 ± 11). We also observed high viability, ~97%, through the direct introduction, whereas the viability was low, ~45%, when the cells were introduced through the microchannels (Figure 2a). We assume that, through direct introduction of cells, the viability was increased owing to the short travel time with the reduced potential damage of cells. The simplicity of our system and the methodology is greatly advantageous compared to that of the existing cell introduction techniques.[48−50] Previously, cell distribution had unintended cell settlement and undesirable cell attachment outside the
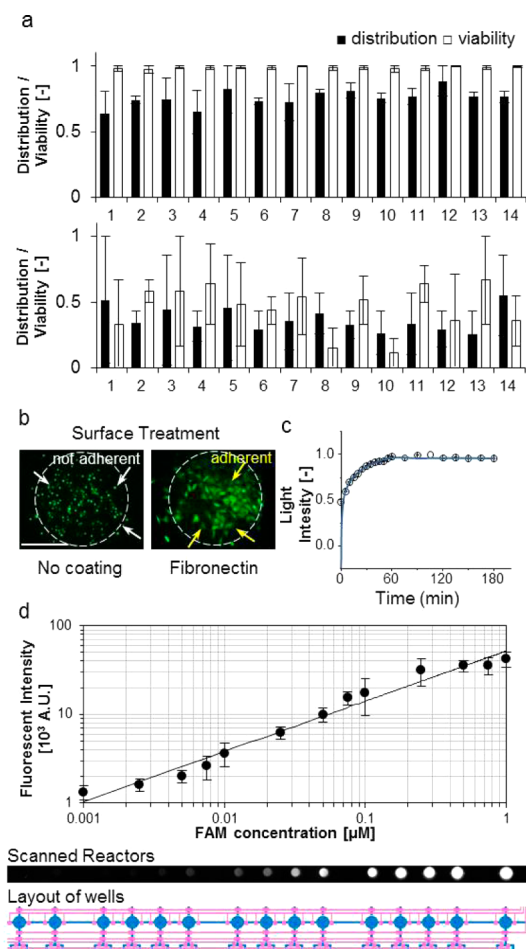
Figure 2. (a) Distribution and viability of cells with direct introduction from the top of the well (upper graph) and introduction through microchannels (bottom). (b) Effect of fibronectin treatment on cell attachment. Yellow arrows indicate adherent cells with surface treatment, while white arrows indicate nonadherent cells without the surface treatment. The scale bar represents 200 μm. (c) Efficiency of mixing with the perilstaltic micromixer. (d) Log–log scale standard curve of fluorescein with the scanned image of FAM gradients in the wells.

areas of interest for cell deposition.[41,48] However, in the present system, cells settled down to the bottom surfaces of the chambers, where they were sequestered with surface treatments for further cytotoxicity tests (Figure 2b).

To characterize the mixing efficiency of the inhibitor and cell culture medium inside the microwell chambers, we introduced color dyes from the mixer into the microwells and measured the light intensity of the dyes over the chamber area. We observed more than 50% mixing during the introduction of the solution into the microwell followed by more than 80% mixing within the next 15 min (Figure 2c). As this paper is an adaptation of the existing gradient former[28,30] on open wells for cytotoxicity tests, we checked that the concentration gradient in the dilution network was effectively realized in the open-well microchambers. We generated a concentration gradient of FAM from 0.01 to 1.00 μM in the 14 microwells and measured their fluorescence intensities. The standard curve, as presented in Figure 2d, shows a linear relationship between the concentration of FAM and the fluorescence intensity.

On-Chip Cytotoxicity Measurement and IC$_{50}$ Determination. To perform cell-based cytotoxicity tests in the

present chip, we measured IC$_{50}$ values from a single experiment repeated three times. After 24 h of cell culture on chip with Triton X-100, H$_2$O$_2$, or CdCl$_2$ at different concentrations (summarized in Table S1, Supporting Information), 3T3 fibroblasts were stained with calcein AM for live cells and propidium iodide (PI) for dead cells. As shown in Figure 3, the viability of cells against Triton X-100 remained above 95% when the surfactant concentration was below 50 μg/mL. Then a drastic decrease was observed with an increase of the Triton X-100 concentration between 100 and 150 μg/mL. When the concentration was higher than 500 μg/mL, we could not detect any live cells. For H$_2$O$_2$, cell viability was about 80% when the concentration was lower than 0.42 mM. The viability was further decreased to lower than 1% when the concentration was increased above 8.44 mM. We observed similar responses with CdCl$_2$. When CdCl$_2$ concentrations were below 0.01 mM, the cell viability was about 75%. Above 0.25 mM CdCl$_2$, viability was less than 5%. To determine the IC$_{50}$ values, live and dead cells were counted and the viability in each well that had a different concentration of a chemical was converted to a relative viability. Then we plotted dose–response curves as functions of log-scale inhibitor concentrations. To validate our system, the values observed on the chip were compared with those obtained with conventional off-chip experiments, as summarized in Table 2. We believe the strong similarity between the on-chip results and the conventional plate-based off-chip results suggests our systems could replace conventional cell experiments. The present microfluidic device and related methodology provide a reliable platform for conducting cytotoxicity evaluations and the determination of IC$_{50}$ values of inhibitors with the automation of sample metering, gradient generation, mixing, cell culture, incubation, and optical detection.

Our microfluidic device can also be used for cellular dose–response analysis and the determination of other cytotoxicity parameters, such as the half-maximal effective concentration, or EC$_{50}$, and the median lethal concentration, or LC$_{50}$, where a wide and logarithmic scale concentration gradient is required. The present device directly holds the capability of investigating the impact of heavy metals, cosmetic agents, pesticides, cleaning agents, nanoparticles, and environmental pollutants on cells. Moreover, less or moderate toxic compounds could be examined in the present system. In this case, one would need a longer exposure time, or an adjustment in the number of cells to pick up events that happen only to a small number of cells due to the less cytotoxic chemicals. In addition, we designed our system to observe the cells directly and change a solution in a well easily. This makes it suitable to investigate other mechanisms of toxicity, apoptosis and cell proliferation, or the physiological state of the cells as a function of different concentrations of soluble factors such as growth factors or cytokines.

■ CONCLUSIONS

In conclusion, we demonstrated a new method of determining cell-based IC$_{50}$ values by using an integrated microfluidic chip consisting of a gradient generation unit and microwell chambers for cell harboring. We showed that the cell-based assays could be performed by using about 100–150 cells and nanoliter-scale inhibitors on the present system. We successfully determined IC$_{50}$ values of three cytotoxic molecules, Triton X-100, H$_2$O$_2$, and CdCl$_2$, on NIH/3T3 fibroblast cells from the corresponding logistic dose–response plots of each inhibitor with single on-chip experiments. Our proposed system
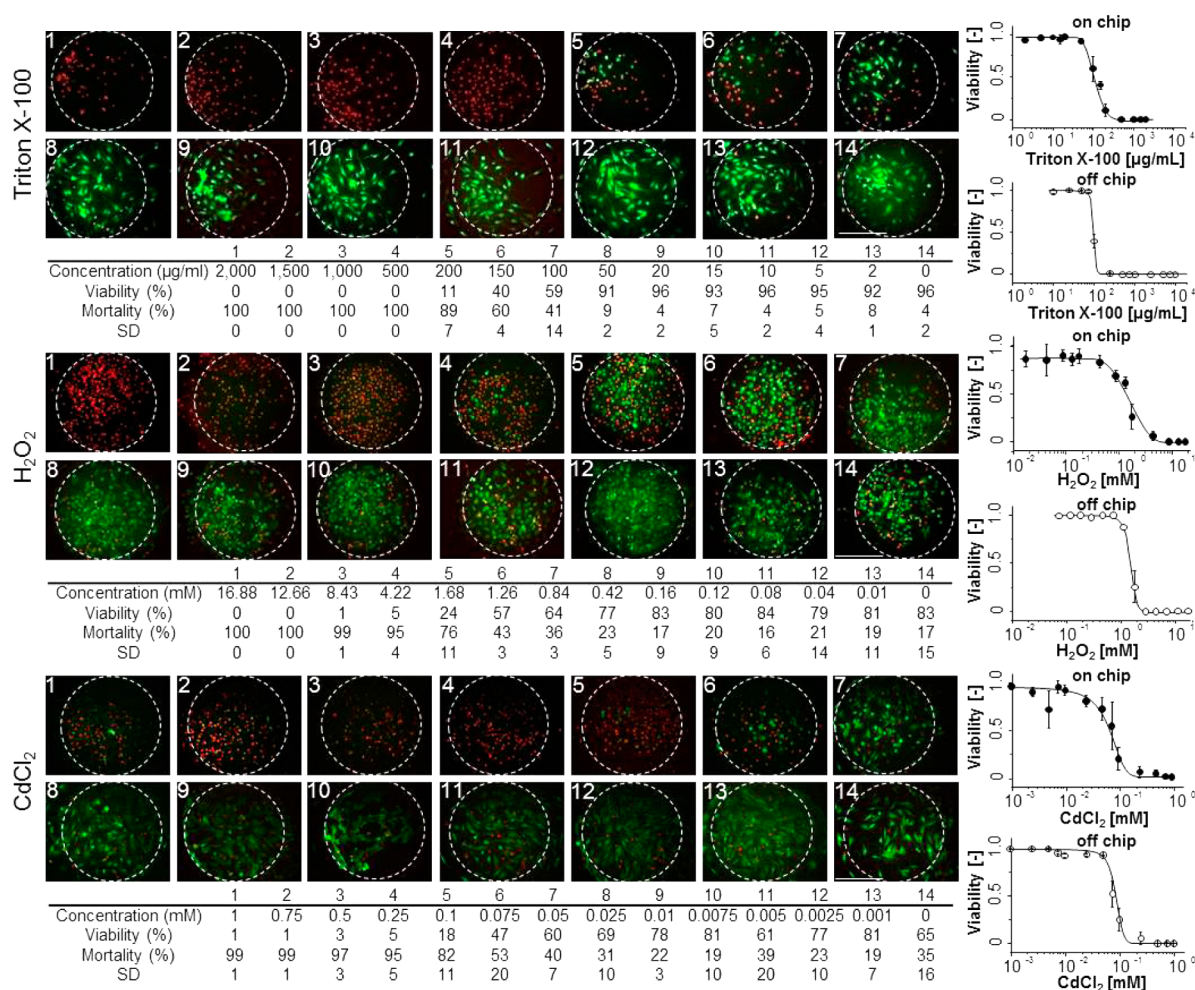
Figure 3. Images of cells from the 14 different open-well microchambers that are integrated to the gradient former. Trion X-100, hydrogen peroxide (H_2O_2), and cadmium chloride ($CdCl_2$) on the NIH/3T3 cell culture were examined. Live cells are stained in green and dead cells in red. The white dotted circle represents the top boundary of each well. The scale bar represents 200 μm. The viability and mortality of the cells in each well are summarized below the pictures. The dose–response curves of each chemical are indicated on the right. Black circles indicate on-chip results and open circles off-chip results.

Table 2. IC$_{50}$ Values of Triton X-100, Hydrogen Peroxide, and Cadmium Chloride[a]

	on chip	off chip	references NIH/3T3	references other cells
Triton X-100 (μg/mL)	120 $\pm$ 10	100 $\pm$ 0	NA	34[b]
H_2O_2 (mM)	1.5 $\pm$ 0.2	1.5 $\pm$ 0.2	NA	0.1–6[c]
$CdCl_2$ (μM)	79 $\pm$ 13	80 $\pm$ 11	NA	15[d]

[a]NA = Not available on NIH/3T3. Results are represented as the mean $\pm$ SD of three independent experiments ($n = 3$). [b]On human fibroblasts.[51] [c]On human skin fibroblasts.[32,33] [d]On BALB/3T3 fibroblasts.[18,21]

is potentially useful for the screening of small molecules on other kinds of cells and observing their effects on cell behaviors. The on-chip IC$_{50}$ values were in close proximity to the IC$_{50}$ values obtained by using 96-well-plate-based conventional methodology. In the area of drug discovery, the present system and methodology could be used to exploit potential new drug candidates quickly and accurately on specific cancer cells, yeasts, or bacterial cells.

■ ASSOCIATED CONTENT

S **Supporting Information**
Additisional information as noted in text. This material is available free of charge via the Internet at http://pubs.acs.org.

■ AUTHOR INFORMATION

Corresponding Author
*E-mail: hongjon@auburn.edu.

Present Address
▽S.J.: Pacific Northwest National Laboratory, Richland, WA 99352.

Notes
The authors declare no competing financial interest.

■ ACKNOWLEDGMENTS

■ REFERENCES

(1) Marx, U., Sandig, V., Eds. *Drug Testing in Vitro: Breakthroughs and Trends in Cell Culture Technology*; Wiley-VCH: Weinheim, Germany, 2007.

(2) Cong, F.; Cheung, A. K.; Huang, S. M. *Annu. Rev. Pharmacol. Toxicol.* **2012**, *10*, 57−78.

(3) Smith, C. *Nature* **2004**, *428*, 225−231.

(4) Geysen, H. M.; Schoenen, F.; Wagner, D.; Wagner, R. *Nat. Rev. Drug Discovery* **2003**, *2*, 222−230.

(5) Gamo, F. J.; Sanz, L. M.; Vidal, J.; de Cozar, C.; Alvarez, E.; Lavandera, J. L.; Vanderwall, D. E.; Green, D. V.; Kumar, V.; Hasan, S.; Brown, J. R.; Peishoff, C. E.; Cardon, L. R.; Garcia-Bustos, J. F. *Nature* **2010**, *465*, 305−310.

(6) Joseph-McCarthy, D.; Baber, J. C.; Feyfant, E.; Thompson, D. C.; Humblet, C. *Current Opin. Drug Discovery Dev.* **2007**, *10*, 264−274.

(7) Bleicher, K. H.; Bohm, H. J.; Muller, K.; Alanine, A. I. *Nat. Rev. Drug Discovery* **2003**, *2*, 369−378.

(8) Mayr, L. M.; Bojanic, D. *Curr. Opin. Pharmacol.* **2009**, *9*, 580−588.

(9) Houghten, R. A.; Pinilla, C.; Blondelle, S. E.; Appel, J. R.; Dooley, C. T.; Cuervo, J. H. *Nature* **1991**, *354*, 84−86.

(10) Wang, W.; Kim, S.-H.; El-Deiry, W. S. *Proc. Natl. Acad. Sci. U.S.A.* **2006**, *103*, 11003−11008.

(11) Chapman, T. *Nature* **2004**, *430*, 109−115.

(12) Yamori, T.; Matsunaga, A.; Sato, S.; Yamazaki, K.; Komi, A.; Ishizu, K.; Mita, I.; Edatsugi, H.; Matsuba, Y.; Takezawa, K.; Nakanishi, O.; Kohno, H.; Nakajima, Y.; Komatsu, H.; Andoh, T.; Tsuruo, T. *Cancer Res.* **1999**, *59*, 4042−4049.

(13) Moreau, A. S.; Jia, X.; Ngo, H. T.; Leleu, X.; O'Sullivan, G.; Alsayed, Y.; Leontovich, A.; Podar, K.; Kutok, J.; Daley, J.; Lazo-Kallanian, S.; Hatjiharissi, E.; Raab, M. S.; Xu, L.; Treon, S. P.; Hideshima, T.; Anderson, K. C.; Ghobrial, I. M. *Blood* **2007**, *109*, 4964−4972.

(14) Chorghade, M. S. *Drug Discovery and Development*; Wiley-Interscience: Hoboken, NJ, 2006.

(15) Gad, S. C. *Drug Discovery Handbook*; Wiley-Interscience: Hoboken, NJ, 2005.

(16) Zhang, X.; Smith, D. L.; Meriin, A. B.; Engemann, S.; Russel, D. E.; Roark, M.; Washington, S. L.; Maxwell, M. M.; Marsh, J. L.; Thompson, L. M.; Wanker, E. E.; Young, A. B.; Housman, D. E.; Bates, G. P.; Sherman, M. Y.; Kazantsev, A. G. *Proc. Natl. Acad. Sci. U.S.A.* **2005**, *102*, 892−897.

(17) Kang, L.; Chung, B. G.; Langer, R.; Khademhosseini, A. *Drug Discovery Today* **2008**, *13*, 1.

(18) Lee, M. Y.; Kumar, R. A.; Sukumaran, S. M.; Hogg, M. G.; Clark, D. S.; Dordick, J. S. *Proc. Natl. Acad. Sci. U.S.A.* **2008**, *105*, 59−63.

(19) Wu, J.; Wheeldon, I.; Guo, Y.; Lu, T.; Du, Y.; Wang, B.; He, J.; Hu, Y.; Khademhosseini, A. *Biomaterials* **2011**, *32*, 841−848.

(20) Sugiura, S.; Edahiro, J.; Kikuchi, K.; Sumaru, K.; Kanamori, T. *Biotechnol. Bioeng.* **2008**, *100*, 1156−1165.

(21) Mahto, S. K.; Yoon, T. H.; Shin, H.; Rhee, S. W. *Biomed. Microdevices* **2009**, *11*, 401−411.

(22) Sugiura, S.; Hattori, K.; Kanamori, T. *Anal. Chem.* **2010**, *82*, 8278−8282.

(23) Tilles, A. W.; Baskaran, H.; Roy, P.; Yarmush, M. L.; Toner, M. *Biotechnol. Bioeng.* **2001**, *73*, 379−389.

(24) Jeon, N. L.; Dertinger, S. K. W.; Chiu, D. T.; Choi, I. S.; Stroock, A. D.; Whitesides, G. M. *Langmuir* **2000**, *16*, 8311−8316.

(25) Walker, G.; Beebe, D. J. *Lab Chip* **2002**, *2*, 131−134.

(26) Meyvantsson, I.; Warrick, J. W.; Hayes, S.; Skoien, A.; Beebe, D. J. *Lab Chip* **2008**, *8*, 717−724.

(27) Puccinelli, J. P.; Su, X.; Beebe, D. J. *JALA* **2010**, *15*, 25−32.

(28) Jambovane, S.; Duin, E. C.; Kim, S. K.; Hong, J. W. *Anal. Chem.* **2009**, *81*, 3239−3245.

(29) Selimovic, S.; Sim, W. Y.; Kim, S. B.; Jang, Y. H.; Lee, W. G.; Khabiry, M.; Bae, H.; Jambovane, S.; Hong, J. W.; Khademhosseini, A. *Anal. Chem.* **2011**, *83*, 2020−2028.

(30) Yun, J. Y.; Jambovane, S.; Kim, S. K.; Cho, S. H.; Duin, E. C.; Hong, J. W. *Anal. Chem.* **2011**, *83*, 6148−6153.

(31) Jambovane, S.; Kim, D. J.; Duin, E. C.; Kim, S.-K.; Hong, J. W. *Anal. Chem.* **2011**, *83*, 3358−3364.

(32) Lee, W. S.; Jambovane, S.; Kim, D.; Hong, J. W. *Microfluid. Nanofluid.* **2009**, *7*, 431−438.

(33) Unger, M. A.; Chou, H.-P.; Thorsen, T.; Scherer, A.; Quake, S. R. *Science* **2000**, *288*, 113−116.

(34) Thorsen, T.; Maerkl, S. J.; Quake, S. R. *Science* **2002**, *298*, 580−584.

(35) Wheeler, A. R.; Throndset, W. R.; Whelan, R. J.; Leach, A. M.; Zare, R. N.; Liao, Y. H.; Farrell, K.; Manger, I. D.; Daridon, A. *Anal. Chem.* **2003**, *75*, 3581−3586.

(36) Hansen, C.; Quake, S. R. *Curr. Opin. Struct. Biol.* **2003**, *13*, 538−544.

(37) Motulsky, H.; Christopoulos, A. *Fitting Models to Biological Data Using Linear and Nonlinear Regression: A Practical Guide to Curve Fitting*; Oxford University Press: New York, 2004.

(38) Fok, S.; Domachuk, P.; Rosengarten, G.; Krause, N.; Braet, F.; Eggleton, B. J.; Soon, L. L. *Biophys. J.* **2008**, *95*, 1523−1530.

(39) Chen, S. Y.; Hung, P. J.; Lee, P. J. *Biomed. Microdevices* **2011**, *13*, 753−758.

(40) Keenan, T. M.; Frevert, C. W.; Wu, A.; Wong, V.; Folch, A. *Lab Chip* **2010**, *10*, 116−122.

(41) Young, E. W. K.; Beebe, D. J. *Chem. Soc. Rev.* **2010**, *39*, 1036−1048.

(42) Wang, Z. H.; Kim, M. C.; Marquez, M.; Thorsen, T. *Lab Chip* **2007**, *7*, 740−745.

(43) Toh, Y. C.; Lim, T. C.; Tai, D.; Xiao, G.; van Noort, D.; Yu, H. *Lab Chip* **2009**, *9*, 2026−2035.

(44) Takayama, Y.; Kotake, N.; Haga, T.; Suzuki, T.; Mabuchi, K. *Conf. Proc.: Annu. Int. Conf. IEEE Eng. Med. Biol. Soc.* **2011**, *2011*, 3613−3616.

(45) O'Neill, A. T.; Monteiro-Riviere, N. A.; Walker, G. M. *Lab Chip* **2009**, *9*, 1756−1762.

(46) Walker, G. M.; Zeringue, H. C.; Beebe, D. J. *Lab Chip* **2004**, *4*, 91−97.

(47) Millet, L. J.; Stewart, M. E.; Sweedler, J. V.; Nuzzo, R. G.; Gillette, M. U. *Lab Chip* **2007**, *7*, 987−994.

(48) Lee, P. J.; Hung, P. J.; Rao, V. M.; Lee, L. P. *Biotechnol. Bioeng.* **2006**, *94*, 5−14.

(49) Jang, Y. H.; Kwon, C. H.; Kim, S. B.; Selimovic, S.; Sim, W. Y.; Bae, H.; Khademhosseini, A. *Biotechnol. J.* **2011**, *6*, 156−164.

(50) Gómez-Sjöberg, R.; Leyrat, A. A.; Pirone, D. M.; Chen, C. S.; Quake, S. R. *Anal. Chem.* **2007**, *79*, 8557−8563.

(51) Arechabala, B.; Coiffard, C.; Rivalland, P.; Coiffard, L. J.; de Roeck-Holtzhauer, Y. *J. Appl. Toxicol.* **1999**, *19*, 163−165.